

UCRL-2544
Unclassified—Chemistry Distribution

UNIVERSITY OF CALIFORNIA

m. O. 43906

Radiation Laboratory

Contract No. W-7405-eng-48B

REACTIONS OF THE REFRACTORY SILICIDES WITH CARBON AND WITH NITROGEN

Leo Brewer and Oscar Krikorian

April 29, 1954

Berkeley, California

REACTIONS OF THE REFRACTORY SILICIDES WITH CARBON AND WITH NITROGEN

Leo Brewer and Oscar Krikorian

Department of Chemistry and Chemical Engineering
and the Radiation Laboratory
University of California, Berkeley, California

April 29, 1954

ABSTRACT

The silicides of Ti, Zr, Ce and Nb were investigated to determine the phases present at temperatures around 2000°K. The reactions of silicides of Ti, Zr, Ce, Nb, Ta, Mo and W with carbon were studied at these temperatures. Also a limited amount of work was done on the reactions of some of the silicides with nitrogen. The data have been used to establish ternary phase diagrams for the systems and to obtain upper and lower limits for the heats of formation of the silicides.

REACTIONS OF THE REFRACTORY SILICIDES WITH CARBON AND WITH NITROGEN

Leo Brewer and Oscar Krikorian

Department of Chemistry and Chemical Engineering
and the Radiation Laboratory
University of California, Berkeley, California

April 29, 1954

INTRODUCTION

The silicides of Ti, Zr, Ce, Nb, Ta, Mo and W were investigated in order to obtain thermodynamic data on their stabilities and thus determine their importance as refractories. These metals are expected to form the most stable silicides from a comparison with the carbide stability region in the periodic table.

The disilicides of the above metals are well known. In addition to these, lower silicides have been reported for Ti, Zr, Nb, Ta, Mo and W. In this work most of the reported silicide phases are confirmed and lower silicide phases are reported for the Ce-Si and Nb-Si systems. The newly found phases are given in Table I. A limited amount of work was also done on the Nb-C and Ce-C systems. New phases that were found are given in Table I.

Combustion calorimetry and solution calorimetry are not easily applicable in determining the heats of formation of silicides due to their inertness toward oxidation and solvents. Dissociation pressure measurements would probably be the most applicable in determining the stabilities of the silicides. Searcy and McNees¹ have determined the stabilities of the rhenium silicides by studies of this type. In order to undertake studies of this type on other refractory silicides, information on the phases present, their approximate stabilities and suitable containers are of great importance.

In this work we have resorted to high temperature equilibrium studies involving silicides in order to obtain useful information about their stabilities. The equilibrium studies involved the systems M-Si, M-Si-C, M-Si-N₂ and M₁-M₂-Si. By comparing the stabilities of the silicides with the corresponding carbides and nitrides it was possible to set upper and lower limits to the stabilities of many of the silicides. The M₁-M₂-Si equilibria gave information about the relative stabilities of the silicides.

EXPERIMENTAL PROCEDURE

The M-Si and M-Si-C and N_1-N_2 -Si reactions were carried out by mixing together 40 to 400 mesh powders of the reactants and heating them in Mo or graphite crucibles in the inductively heated equipment described by Brewer, Bromley, Gilles and Lofgren.² Mo crucibles were found to be satisfactory containers since in most cases the Mo silicides were less stable than those of the other metals studied. In those cases in which the sample silicides were less stable than the Mo silicides, crucible attack still did not occur providing that the samples did not fuse. A protective silicide layer on the surface of the Mo evidently prevented further attack. Graphite crucibles were used when the samples contained graphite in excess. Usually equilibrium was rapidly established between the reactants which then sintered and drew away from the container.

Cerium metal powder could not be used because of the oxidation problem. Therefore the cerium silicide samples were prepared by allowing small pieces of cerium metal rod to react with silicon or silicon plus graphite powders.

Most of the reactions were carried out at about 2100°K. In the case of the samples containing cerium the heatings were carried out at 1600°K. Three fourths of an atmosphere of argon was used in the systems to suppress volatilization of the Si.

The M-Si- N_2 systems were studied by allowing metal and silicon powder mixtures to come into equilibrium with N_2 gas at about 3/4 atm pressure and at various temperatures. When sintering took place in the samples it was not certain that the sample was homogeneous throughout. For this reason it was found to be necessary to introduce N_2 into the samples in the form of Si_3N_4 . Mo containers were again used for most of the heatings. However Mo containers

were found not to be satisfactory in the case of the Ti and Zr systems because of crucible attack. ZrO_2 containers were also used for these systems but there is some question about reaction of the ZrO_2 with the silicon of the sample.

The samples were quenched by turning off the induction heater and allowing the samples to cool in the presence of Ar or N_2 . It required about three minutes for the samples to cool from 2100 to 1200°K.

X-ray powder diffraction patterns were taken of the resulting samples. Copper K_α radiation was used for identification of samples and chromium K_α radiation used when measurement of lattice parameters was involved.

Temperatures were measured with optical pyrometers calibrated with a standardized tungsten filament lamp obtained from the National Bureau of Standards. The samples were sighted through an optical glass window which was protected by a metal shield from any material effusing from the furnace when readings were not being taken. The appropriate window corrections were applied to the temperature readings.

STARTING MATERIALS

The silicon metal was obtained from the J. T. Baker Chemical Company in the form of lumps. It was ground to finer than 140 mesh with a steel mortar and pestle. Spectroanalysis showed the main impurities to be: Ti less than 1%, Cr 0.1-1% and Al and Fe approximately 0.1%. X-ray analysis showed a very weak unidentified second phase.

The Zr metal was obtained in the form of high purity sponge and of rather impure powder. The main impurities in the powder were dissolved oxygen and nitrogen. X-ray diffraction showed two Zr phases—one set of lines corresponding to pure Zr and the other to Zr with dissolved O or N. The phase with the expanded lattice ($a = 3.26 \text{ \AA}$, $c = 5.19 \text{ \AA}$) corresponds to 22 atomic % oxygen assuming that all of the dissolved gas is oxygen.³

Ignition experiments showed that the Zr contains 21.4 atomic % (4.54 wt. %) oxygen. The value from the ignition experiments is taken to be correct.

X-ray analysis of the Ti metal showed that it also contained dissolved oxygen and nitrogen. Assuming that all of the dissolved gas is oxygen the lattice constants ($a = 2.95 \text{ \AA}$, $c = 4.69 \text{ \AA}$) indicate 4.5 atomic percent oxygen.⁴

The main impurity in the Ce metal was 5 atomic % carbon.

All of the other metals were of 99.9% or greater purity.

BINARY SYSTEMS

Brewer, Searcy, Templeton and Dauben⁵ have investigated the Ta-Si, Mo-Si and W-Si systems for the phases present at the temperatures of interest in this investigation. The phases TaSi_2 , $\text{TaSi}_{0.6}$, $\text{TaSi}_{0.4}$, and $\text{TaSi}_{0.2}$ were found in the Ta-Si system. In the Mo-Si system the phases MoSi_2 , Mo_3Si_2 ($\text{MoSi}_{0.65}$), and Mo_3Si were found. The W-Si system showed the phases WSi_2 and $\text{WSi}_{0.7}$.

In an x-ray investigation of Ta-Si system by Nowotny, Schachner, Kieffer and Benesovsky,⁶ structures were assigned to phases $\text{Ta}_{4.5}\text{Si}$, Ta_2Si and Ta_5Si_3 . The x-ray pattern found for $\text{Ta}_{4.5}\text{Si}$ was different than for the $\text{TaSi}_{0.2}$ reported by Brewer et al. These two phases may be high and low temperature forms of the same compound. Ta_2Si corresponds to the $\text{TaSi}_{0.4}$ of Brewer et al. The Ta_5Si_3 pattern however is different than for the $\text{TaSi}_{0.6}$ phase reported by Brewer et al. The two phases may again be high and low temperature modifications or, as will be discussed later, the Ta_5Si_3 phase may have been stabilized by graphite.

In this work the systems Ti-Si, Zr-Si, Ce-Si and Nb-Si were investigated for the phases present at high temperatures. The results of these heatings are presented in Tables II-VI. The symbols s. (strong), m.s. (moderately strong), m. (moderate), m.w. (moderately weak), w. (weak) and v.w. (very weak) refer to the observed x-ray intensities. The final temperature before quenching has been given in the tables. If the annealing temperature exceeded the final temperature before quenching by more than 25° then the maximum temperature attained is also given. No containers were used for all of the heatings unless otherwise indicated. Any evidence of melting of the sample has also been indicated. In all cases that the samples fused, they had a silvery-gray metallic luster.

Ti-Si System. In addition to $TiSi_2$, the Ti_5Si_3 phase reported by Pietrokowsky and Duwez⁷ was found. At 2105°K, a sample containing 30.0% Si melted, a sample containing 33.5% Si was sintered and a sample containing 37.5% Si was partially melted. This shows that the sample at 33.5% Si falls within the homogeneity range of Ti_5Si_3 . The lattice constants of Ti_5Si_3 were visually observed to vary continuously as we went from 20% to 60% Si. They were largest at 20% and smallest at 60% Si. This effect is partly due to the homogeneity range of Ti_5Si_3 , partly due to the presence of a small amount of oxygen in the Ti starting material, and may also be partly due to Mo dissolving in the Ti_5Si_3 lattice. The lattice constants of Ti_5Si_3 in the sample containing 37.5% Si were measured and found to be $a = 7.419 \pm 0.007$ A and $c = 5.135 \pm 0.007$ A as compared to $a = 7.465 \pm 0.002$ and $c = 5.162 \pm 0.002$ reported by Pietrokowsky and Duwez.⁷

The $TiSi$ phase reported by Hansen, Kessler and McPherson⁸ was not definitely observed. Many weak lines appeared in the $TiSi$ region along with Ti_5Si_3 . These lines appear to be due to several phases, one of which may correspond to the $TiSi$ reported by Hansen et al. $TiSi_2$ and Ti_5Si_3 were found together in one sample indicating that any intermediate phases must have disproportionated upon quenching.

Attack of the crucible by a sample containing 67% Si showed that Mo is capable of reducing $TiSi_2$ to Ti_5Si_3 . Also the presence of Mo in fused samples of Ti_5Si_3 indicates that Ti_5Si_3 is stable in the presence of Mo.

Zr-Si System. Lundin, McPherson and Hansen⁹ have reported the phases $ZrSi$, Zr_6Si_5 , Zr_4Si_3 , Zr_3Si_2 , Zr_2Si and Zr_4Si in addition to the previously known $ZrSi_2$. The phases were identified by metallographic analysis. X-ray analysis was also applied to a limited extent. X-ray diffraction studies by Schachner,

Nowotny and Machenschalk¹⁰ on the Zr-Si system have indicated that the phase Zr_5Si_3 with the Mn_5Si_3 structure is the only phase present in the region between Zr_2Si and $ZrSi$. Samples containing the lower silicides were supplied to us by Dr. McPherson for comparison with our phases.

X-ray analysis of Dr. McPherson's samples showed characteristic patterns for the reported phases. The best Zr_4Si pattern was found in a picture which also contained Zr. Zr_2Si appeared along with a small amount of Zr_4Si . Zr_3Si_2 appeared in single phase. It was found to have the Mn_5Si_3 structure with the lattice constants $a = 7.958 \pm .005A$, $c = 5.564 \pm .005A$. Zr_5Si_3 is probably a more appropriate designation for this phase in associating it with its structure. In comparing the lattice constants for Zr_5Si_3 here with those in our work we found that the values did not agree. This is an indication of a large homogeneity range for Zr_5Si_3 . The Zr_4Si_3 and Zr_6Si_5 phases appeared in what seemed to be single phase. The $ZrSi$ phase agreed well with our $ZrSi$ samples, however it appeared to have a few extra lines. Our work showed that $ZrSi$ does not index well on the hexagonal lattice reported by Lundin et al.

For preparing our compounds of Si with pure Zr, small pieces of the sponge Zr were first allowed to react with Si metal powder for an hour at 1952°K. Some of the samples were then powdered to 140 mesh or finer and reheated.

During the first heating a sample containing 22.4% (8.17 wt %) Si fused with no apparent crucible attack. The x-ray pattern was not identified with any of the known phases. It appeared to be single phase and may be a high temperature form of Zr_4Si . At 35% Si, Zr_2Si appeared in single phase. Zr_2Si was also found in the remaining samples ranging up to 50% Si under non-equilibrium situations. The lattice parameters of Zr_2Si in the presence of

Zr_5Si_3 were found to be $a = 6.646 \pm .008A$ and $c = 5.300 \pm .008A$ according to the tetragonal structure established by Schachner et al.¹⁰ Upon powdering and reheating the samples containing from 40 to 50% Si, the Zr_2Si disappeared. At 40% Si the phase Zr_5Si_3 appeared. At 45% Si Zr_5Si_3 appeared along with Zr_4Si_3 and Zr_6Si_5 and at 50% Si, Zr_5Si_3 appeared along with Zr_6Si_5 and $ZrSi$. Although equilibrium was not completely established, the Zr_6Si_5 and Zr_4Si_3 phases were confirmed.

In the heatings with the impure Zr powder, $ZrSi$ and Zr_5Si_3 were obtained as single phases while patterns for Zr_4Si_3 and Zr_6Si_5 were indicated but could not be positively identified due to the presence of large amounts of Zr_5Si_3 and $ZrSi$ in that region.

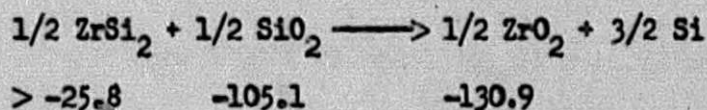
These results indicate that the absence of the Zr_6Si_5 and Zr_4Si_3 phases in the work of Schachner et al.¹⁰ may be due to the presence of an impurity such as O or C. The Zr_5Si_3 may be able to absorb sufficient oxygen or carbon so that the Zr_6Si_5 and Zr_4Si_3 phases disproportionate due to decreased Zr activity in the Zr_5Si_3 phase. Our work on the Zr-Si-C diagram shows that C does indeed dissolve in Zr_5Si_3 .

Zr_2Si and Zr_4Si were not found at 2000°K when the Si content was lower than required for Zr_5Si_3 . Instead Zr_5Si_3 appeared in equilibrium with Zr metal having a largely expanded lattice. However at 1700°K a sample containing 19% Si showed the phase Zr_2Si in equilibrium with Zr. The presence of oxygen evidently affects the stability of the Zr_4Si and Zr_2Si phases by lowering the Zr activity sufficiently so that they disproportionate. As the solubility of oxygen in Zr decreases with temperature the activity of Zr increases. At 1700°K the activity of Zr has increased sufficiently to stabilize the Zr_2Si phase. The presence of oxygen in this system also

raises the eutectic temperature in the Zr-Zr₅Si₃ region. At 2000°K, the samples in this region were well sintered and were probably close to the eutectic temperature.

Samples containing more than 50 atomic % Si were attacked by the crucible if allowed to fuse. ZrSi and MoSi₂ were the resultant phases indicating that Mo is capable of reducing ZrSi₂ to ZrSi.

Experiments were done by William Hicks¹¹ to check the stability of the silicides in the presence of ZrO₂. When ZrO₂ was heated with Zr and Si in the mole ratio of 1:1:2 the phases ZrO₂ and ZrSi₂ were found. ZrO₂ was also heated with Si in the ratios of 1:1 and 1:2. Here the phases ZrO₂ and ZrSiO₄ appeared; however, Si metal was not found in the pictures. The absence of Si may be due to the sample picking up oxygen during the heating, or ternary compound formation between ZrO₂ and Si. Assuming that the latter is not the case, the results show that Si and ZrSi₂ as well as ZrSi, Zr₆Si₅, Zr₄Si₃ and Zr₅Si₃ are stable in the presence of ZrO₂. According to this the following reaction will proceed as written:



Assuming that $\Delta S_{298}^\circ = 0$ and $\Delta C_p = 0$ for the reaction and using Brewer's¹² values for the heats of formation of the oxides we calculate an upper limit of $\Delta H_{298}^\circ > -25.8$ kcal. per equivalent of Si for ZrSi₂.

Ce-Si System. The Ce-Si samples were prepared as previously described. They all had the appearance of being fused or partially fused. It was not possible to determine visually the extent of the fusion. There was no evidence of any crucible attack in any of the samples.

The samples were prepared for x-ray analysis by grinding them to 200 mesh in a dry box under argon and sealing the specimens in thin wall glass capillary tubes.

Due to the method of preparation the samples were inhomogeneous mixtures. However, it was established that several lower silicides exist. These are provisionally assigned the formulas Ce_3Si , Ce_2Si and $CeSi$.

The Ce_3Si phase appeared along with CeO_2 in all of its samples. The CeO_2 probably came about from oxidation of Ce metal during preparation of the specimens for x-ray study in spite of the precautions. Therefore, it is believed that Ce_3Si is the lowest silicide.

The Ce_2Si appeared in samples containing 32 to 36% Si and $CeSi$ appeared in samples containing 38 to 49% Si. $CeSi$ appears to have the USi structure.

$CeSi_2$ was obtained in single phase and its lattice constants were measured. $CeSi_2$ is reported to have the tetragonal $ThSi_2$ ¹³ type structure with the lattice constants $a = 4.16 \pm .03A$, $c = 13.90 \pm .07A$.¹⁴ We obtained the more accurate values, $a = 4.175 \pm .002A$, $c = 13.848 \pm .006A$. It should be remembered however, that our original Ce starting material contained 5 atomic % C.

Nb-Si System. The Nb-Si system showed the two lower silicides $NbSi_{0.55 \pm 0.1}$ and Nb_5Si_3 . $NbSi_{0.55}$ is isostructural with the $TaSi_{0.6}$ phase reported by Brewer et al.⁵ It was obtained in equilibrium with Nb metal up to 36% Si. The Nb_5Si_3 is of the Mn_5Si_3 type structure. Nb_5Si_3 in equilibrium with $NbSi_2$ gave the lattice constants, $a = 7.547 \pm .005A$, $c = 5.240 \pm .005A$. The sample richest in Nb_5Si_3 contained what seemed to be a small amount of $NbSi_{0.55}$ plus a phase isostructural with the $WSi_{0.7}$ ⁵ previously reported. On the higher

silicon side Nb_5Si_3 was found in equilibrium with $NbSi_2$. Since Nb_5Si_3 and $NbSi_{0.6}$ were not obtained in equilibrium with each other, other silicides may exist in the region between $NbSi_{0.55}$ and Nb_5Si_3 .

The samples that were held at 2095°K for 13 minutes were not quenched rapidly but required about 12 minutes to cool to 1200°K. Several of these samples showed Nb, $NbSi_{0.55}$ and Nb_5Si_3 in the presence of each other. However, this non-equilibrium condition is probably due to inhomogeneity of the samples rather than a temperature effect.

In an x-ray investigation of the Nb-Si system, Brauer and Scheele¹⁵ found that two forms of Nb_2Si (α and β) exist which seem to be separated by a small homogeneity range. These two phases evidently are our $NbSi_{0.55}$ and Nb_5Si_3 phases. The presence of a homogeneity range joining these two phases remains to be confirmed.

A sample containing 31% Si fused at 2231°K whereas none of the samples containing 31% or less of Si fused at 2095°K. Therefore the Nb- $NbSi_{0.55}$ eutectic must lie at $2160 \pm 70^\circ K$. The sample containing 50% Si fused at 2132°K while no fusion was observed at 2095°K for the sample containing 66% Si setting the Nb_5Si_3 - $NbSi_2$ eutectic at $2110 \pm 30^\circ K$.

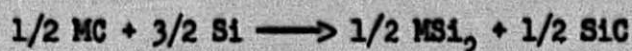
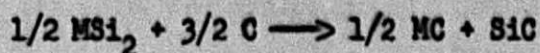
Since there was no evidence of crucible attack, except in a sample containing silicon in excess of $NbSi_2$, it appears that Mo cannot reduce any of the Nb silicides.

M-Si-C SYSTEMS

If the heats of formation of the carbides in these systems are known, then it is possible to obtain limits on the heats of formation of the silicides. In order to make these calculations, use is made of the approximate relation:

$$\Delta F_T^\circ = \Delta H_{298}^\circ - T\Delta S_{298}^\circ$$

We assume that ΔS_{298}° is zero when all reactants and products are solids. Heats of formation of the carbides will then suffice to set limits for the heats of formation of the silicides. As an example of the method used, consider the reactions:



If we take the ΔH_{298}° of formation of SiC as -13.0 kcal.^{16} and that of MC as A, then ΔH_{298}° of formation for MSi_2 must be greater than $(1/2 A - 13.0) \text{ kcal.}$ and less than $(1/2 A + 13.0) \text{ kcal.}$ for the reactions to go as written.

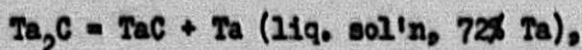
The values of the heats and entropies of formation of the carbides used in these calculations have been tabulated in Table VII.

The entropy values for SiC, TiC and TaC are the third law values obtained from Kelley.¹⁷ Entropies for the other carbides were estimated by Latimer's method.¹⁸ The assignments for the entropy contribution of C in a solid compound were obtained by subtracting the contribution of the metal from the known entropies of carbides¹⁷ (see Table VIII). It was found that about -4.1 e.u. may be assigned to C for its contribution in a carbide of one to one metal to carbon ratio, about -7.2 e.u. in a carbide of two to one or three to one metal to carbon ratio and about -14 e.u. in a carbide of four to one metal to carbon ratio.

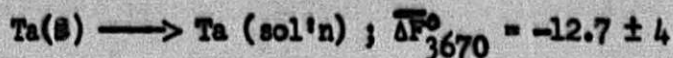
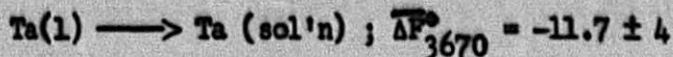
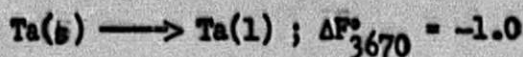
The absolute entropy of WC for example, is estimated as $S^\circ = S_M^\circ + S_C^\circ = 15.0 - 4.1 = 10.9$ e.u. Using values of 8.04, and 1.36 e.u.¹⁷ for the absolute entropies of W and C respectively, ΔS_{298}° of formation for WC is estimated as 1.5 ± 1 e.u.

The value for the heat of formation of SiC was obtained from the work of Humphrey, Todd, Coughlin and King.¹⁶ The heats of formation for TiC and TaC are from the work of Humphrey^{19,20} and the value for WC is from Huff, Squitieri and Snyder.²¹

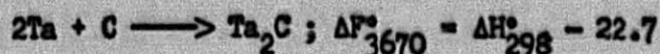
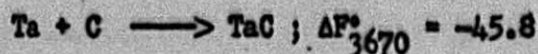
Use was made of the equilibrium



which exists at 3670°K ²² to calculate the value for the heat of formation of Ta_2C . The activity of liquid Ta in this solution is estimated to be 0.2 ± 0.1 . This estimation is made realizing that for TaC rich in graphite the activity of liquid Ta is very small. The entropy and heat of fusion of Ta have been given by Brewer²³ as 2.3 e.u. and 7.5 kcal. per mole respectively. Using these data we calculate,



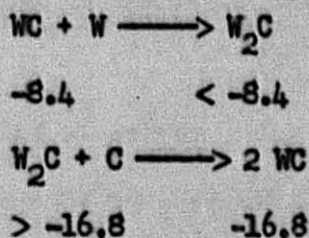
Estimating average ΔC_p 's of formation over a temperature range of 298 to 3670°K to be 2 and 3 cal.deg.⁻¹ mole⁻¹ respectively for TaC and Ta_2C , we calculate,



Combining the expressions we find that ΔH_{298}° of formation for Ta_2C is -36 ± 8 kcal. per mole.

The values for the heats of formation of Mo_2C and MoC were calculated from the equilibrium constant data of Browning and Emmett²⁴ for the reactions $2Mo + CH_4 = Mo_2C + 2H_2$ and $Mo_2C + CH_4 = 2MoC + 2H_2$. In making these calculations the S_{298}° for Mo_2C and MoC were estimated by the method described above. The heat capacity of MoC was estimated to be 2/5 the heat capacity of Cr_3C_2 ,²⁵ that for Mo_2C was assumed to be 3/10 the heat capacity of Cr_7C_3 .²⁵ The estimated values were combined with the thermodynamic data for the other substances^{25,17} involved in the reaction to tabulate $(\Delta F_T^\circ - \Delta H_{298}^\circ)/T$ functions for the reactions. ΔH_{298}° was found to be 13.67 ± 1.09 kcal. for the first reaction and 18.11 ± 0.20 kcal. for the second reaction. Using the value of -17.89 kcal. per mole for ΔH_{298}° of formation for methane²⁶ we find that ΔH_{298}° of formation is -4.22 ± 1.09 kcal. for Mo_2C and -2.00 ± 0.65 kcal. for MoC .

Limits were set up for the stability of W_2C from a consideration of the reactions:



If we assume that ΔS is approximately 0 for these reactions then ΔH_{298}° of formation for W_2C is less than -8.4 kcal. and greater than -16.8 kcal. We therefore estimate the ΔH_{298}° of formation to be -13 ± 4 kcal.

The ternary diagrams of Figures I to VI have been used to show the phases resulting from the M-Si-C heatings. Several of the diagrams were not completed but the joins that were established are indicated. The Mo-Si-C

system is the most complete. An attempt has been made to give the general form of the melting region along with several ternary eutectic temperatures. The melting diagram of the molybdenum-silicon system has been given by Kieffer and Cerwenka²⁷ and the molybdenum-carbon diagram has been summarized by Hansen.²⁸

No crucibles were used in all of the heatings except for a few samples in the Mo-Si-C and W-Si-C systems which were rich in C. Graphite crucibles were used for these. Crucible attack was observed only in the Ti-Si-C system. Strong attack in one of the samples showed the phases MoSi_2 , Ti_5Si_3 and TiC .

Ternary compounds were observed in the Zr-Si-C, Nb-Si-C, Ta-Si-C and Mo-Si-C systems while there was no indication of ternary compounds in the Ti-Si-C and W-Si-C systems. The ternary compounds all appeared to be like the Mn_5Si_3 structure.

Only a limited amount of work was done on the Zr-Si-C system. The ternary compound that is formed is believed to be due to the solubility of C in Zr_5Si_3 .

In the Ce-Si-C system a sample containing 25% Ce, 50% Si and 25% C was held at 1605°K for 44 minutes. The resultant phases were CeSi_2 plus an unidentified phase. The sample was gray-brown in color and gave off an acetylene odor.

An investigation of the Ce-C system in the range between 50% and 67% C showed the phases CeC , Ce_2C_3 and CeC_2 plus several unidentified phases. None of these phases could be identified in the Ce-Si-C sample. The Ce_2C_3 was identified as being isomorphous with Pu_2C_3 which has a body centered cubic structure.²⁹ CeC is of the NaCl face-centered cubic structure.²⁹ (see Table I). The Ce-C samples were a golden brown in color.

The ternary compound in the Nb-Si-C system, $\text{Nb}_5\text{Si}_3\text{C}_x$, is of the same structure as Nb_5Si_3 , however the lattice constants are considerably different for the two indicating that a large homogeneity range exists for Nb_5Si_3 in the presence of C.

A hexagonal phase isomorphous with Ta_2C was observed in the Nb-Si-C system indicating the presence of an Nb_2C phase. An attempt was made to prepare pure Nb_2C . A powder mixture of 67% Nb and 33% C was held at 2130°K for 38 minutes in a Mo crucible under vacuum. The result was the phases Nb_2C and NbC in equilibrium. Similar treatment of a mixture of 75% Nb and 25% C at 1920°K showed Nb_2C as the principle phase with a very small amount of NbC present. The lattice constants of Nb_2C in equilibrium with NbC are given in Table I. An Nb_2C phase has been mentioned previously in the literature.^{30,31}

In the Ta-Si-C system the ternary compound appeared in single phase in a sample corresponding to the composition $Ta_{4.8}Si_3C_{0.5}$. No variation in lattice constants was observed in the x-ray patterns, so that there is no evidence for an extended homogeneity range.

The Mn_5Si_3 structure has two molecules per unit cell. Assuming that the carbons in $Ta_{4.8}Si_3C_{0.5}$ are interstitial and the departure of the number of Ta's from 5 is due to vacancies in the lattice, we calculate an x-ray density of 12.48 gm/cm³ for $Ta_{4.8}Si_3C_{0.5}$. The density of the powder measured with a pycnometer using the volume displacement of CCl_4 gave 12.4 gm/cm³.

Nowotny, Schachner, Kieffer and Benesovsky⁶ report a phase Ta_5Si_3 of the Mn_5Si_3 structure in the Ta-Si system with the lattice constants $a = 7.474\text{\AA}$, $c = 5.225\text{\AA}$ and $a/c = 1.430$. These values are close to those which we obtained for $Ta_{4.8}Si_3C_{0.5}$. In the work on the Ta-Si system by Brewer et al,⁵ Ta_5Si_3 with the Mn_5Si_3 structure was not found although a phase of composition $TaSi_{0.6}$ was found which did not have the Mn_5Si_3 structure.

Nowotny et al also report that Ta_5Si_3 transforms to a new phase somewhere between 1600 and 1800°K. The new phase observed may be the $TaSi_{0.6}$ reported by Brewer et al. It is possible that carbon from their containers

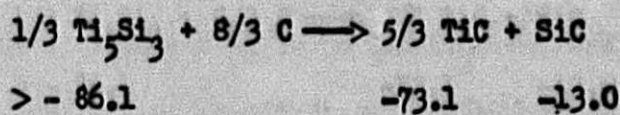
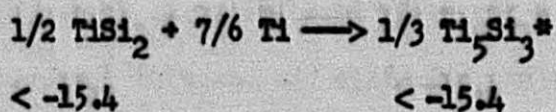
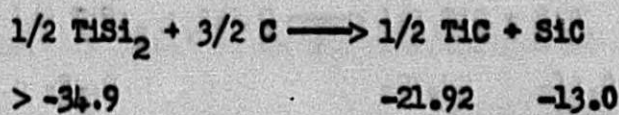
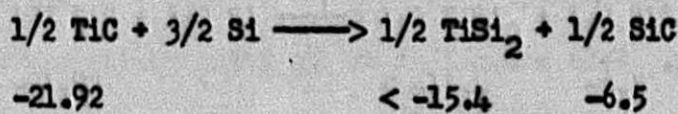
has stabilized the Mn_5Si_3 structure to give the $Ta_{4.8}Si_3C_{0.5}$ phase. This would account for the apparent difficulty of fixing the temperature of transformation.

A variation of lattice constants was observed for $TaSi_2$ as we went from the $TaSi_2$ -SiC-Si region to the $TaSi_2$ -SiC-TaC region indicating solubility of C in $TaSi_2$.

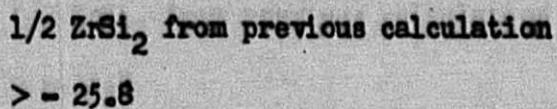
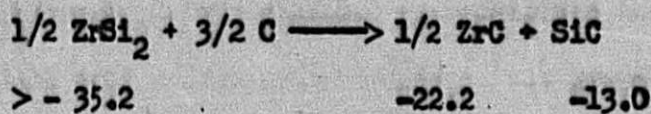
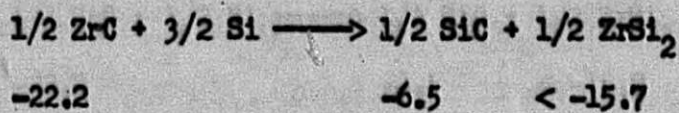
In the Mo-Si-C system a ternary compound was observed at about the composition Mo_4CSi_3 . Considerable variation of lattice parameters with composition was observed for the ternary compound. Evidently C replaces Mo in a Mo_5Si_3 lattice until the composition Mo_4CSi_3 is obtained on the high C side. Lattice constants for the composition Mo_4CSi_3 are $a = 7.285 \pm .007$ and $c = 5.242 \pm .007$.

Using these lattice constants we calculate an x-ray density of 6.62 gm/cm³ for Mo_4CSi_3 and 7.94 gm/cm³ for Mo_5Si_3 . The measured density for a single phase sample of Mo_4CSi_3 was found to be 6.9 gm/cm³ which gives fair agreement with its composition. The homogeneity range for the compound is believed to extend to lower C contents but will not reach the binary Mo-Si region. This phase is the only molybdenum silicide that we have found that is stable in the presence of graphite.

Details on the calculations of the stabilities of the silicides from data of the M-Si-C systems follow. The pertinent results are summarized in Table IX. The numbers below each species are the values for ΔH_{298}° of formation expressed in kilocalories.

Ti-Si-C System:

*Realizing that when lower silicides are stable with respect to disproportionation, they must be more stable per equivalent of Si than the next higher silicide; we will not repeat this type of calculation for the forthcoming silicides.

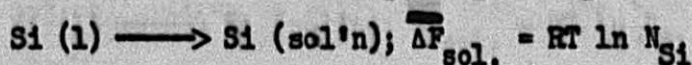
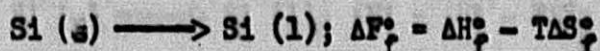
Zr-Si-C System:

Therefore, ΔH_{298}° of formation for $1/2 \text{ ZrSi}_2 = -21 \pm 5 \text{ kcal.}$

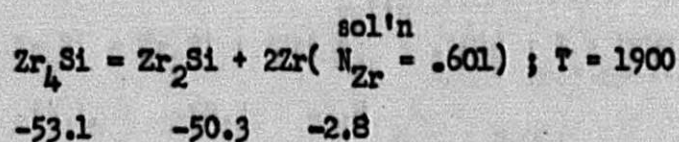
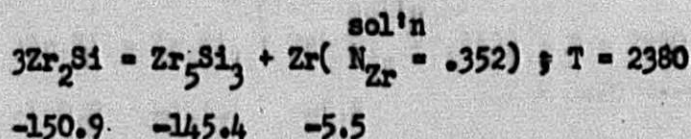
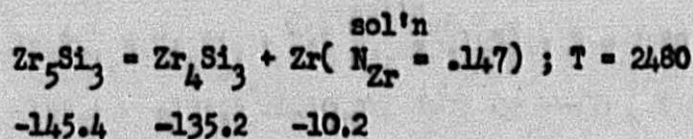
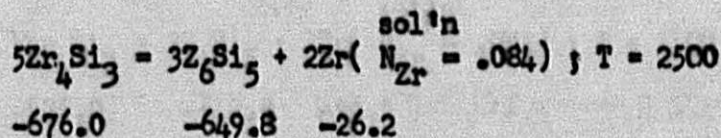
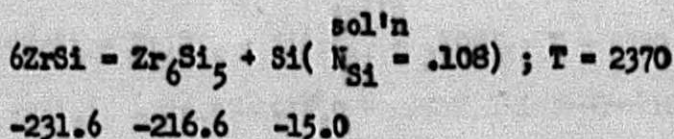
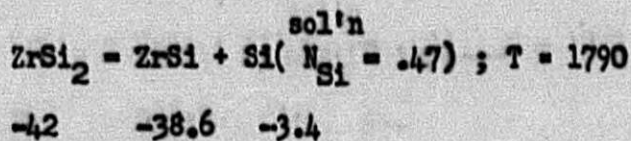
Referring to the Zr-Si phase diagram established by Lundin et al.,⁹ we see that all of the zirconium silicides with the exception of Zr_6Si_5 have incongruent melting points. This means that at the $ZrSi_2$ peritectic we find $ZrSi_2$, ZrSi and a Si rich melt in equilibrium; at the ZrSi eutectic we find ZrSi, Zr_6Si_5 and a Si rich melt in equilibrium; and so on until we find Zr_2Si , Zr_4Si and a Zr rich melt in equilibrium.

If we can estimate the activity of Si or of Zr in the melt at the peritectic points, then we can calculate the heats of formation of all of the other zirconium silicides from the heat of formation of $ZrSi_2$.

We estimate that the activity of Si in the melt is roughly equal to the mole fraction of Si between the stable solid compound and pure Si, when we are working on the Si rich side of the diagram. The free energy of solution of Si from its standard state can then be calculated.

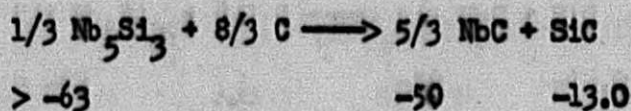
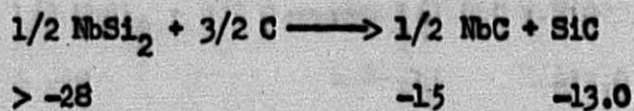
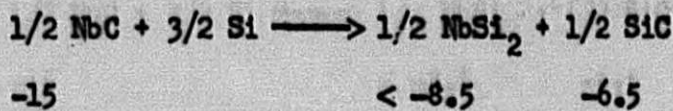


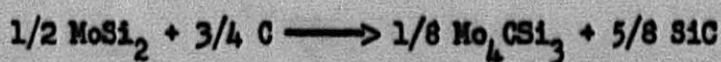
On the Zr rich side of the diagram a similar calculation is made referring to the activity of Zr rather than Si. In these calculations ΔS_f° is taken as 2.3 e.u. for Si^{23} and 6.6 e.u. for Zr^{23} , ΔH_f° is taken as 11.1 kcal. for Si^{23} and calculated as 4.9 kcal. for Zr from the melting point of Zr given by Lundin et al.⁹ In the calculations that follow the numbers below the Si and Zr solutions represent the $\overline{\Delta F}_T$ of solution.



Nb-Si-C System:

The heat of formation of NbC is estimated as ~~-3015~~ kcal. per mole from a comparison with the known heats of formation of the other carbides in this region of the periodic table.



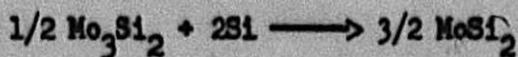


$$A \qquad \qquad \qquad B < -3.5 \qquad \qquad -8.1$$

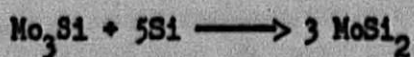


$$B \qquad \qquad \qquad A \qquad \qquad -1.6$$

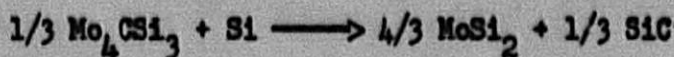
Estimate B = -10.0, then A < -8.4 and > -18.1



$$> -54.3 \qquad \qquad \qquad > -54.3$$

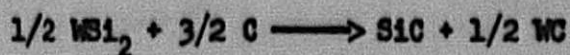


$$> -108.6 \qquad \qquad \qquad > -108.6$$

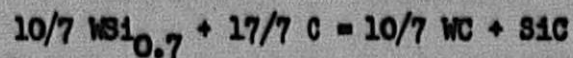


$$> -52.6 \qquad \qquad \qquad -48.3 \qquad \qquad -4.3$$

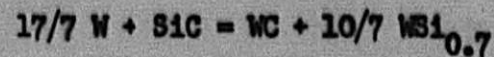
W-Si-C System:



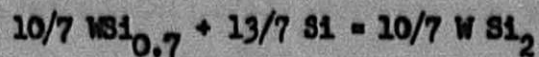
$$> -17.2 \qquad \qquad \qquad -13.0 \qquad \qquad -4.2$$



$$> -25.0 \qquad \qquad \qquad -12.0 \qquad \qquad -13.0$$



$$-13.0 \quad -8.4 \quad < -4.6$$



$$< -4.6 \qquad \qquad \qquad < -4.6$$

M-Si-N₂ SYSTEMS

The M-Si-N₂ systems will give us information about the stabilities of silicides of Ti, Zr, Ce, Nb and Ta since these elements form stable nitrides at high temperatures. The nitrides of these metals may be more stable than the silicides at lower temperatures but at high temperatures the nitrides become less stable due to their positive entropy of formation. Determination of the temperature at which this reversal of stabilities occurs would be very valuable in fixing the stabilities of the silicides.

ΔH_{298}° and ΔS_{298}° of formation data for the nitrides are presented in Table I. The entropy data for Si₃N₄, TiN and ZrN are from Kelley.¹⁷ The other entropies have been estimated. The ΔH_{298}° values for Si₃N₄, CeN, TaN and NbN are from Brewer, Bromley, Gilles and Lofgren,²³ TiN from Humphrey¹⁹ and ZrN from Kelley.³²

Chiotti³³ has shown that the hexagonal structure previously reported for TaN really belongs to the phase Ta₂N. Ta₂N, he found, is the stable species at 2270°K. Upon heating Ta metal under one atm N₂ at 1170°K for 18 hours, Chiotti obtained a composition TaN_{0.9} which contained Ta₂N plus a new phase.

Slade and Higson³⁴ made two measurements on the dissociation pressure of TaN at around 1500°K. From the results of Chiotti we see that they were studying the equilibrium



Estimating ΔS_{298}° for the reaction to be 22 e.u. and $\Delta C_p = 0$, we calculate an average ΔH_{298}° of 43.8 kcal. for the reaction. This yields a value of -72.4 ± 5 kcal. for ΔH_{298}° of formation of Ta₂N.

An experimental difficulty was encountered in attaining equilibrium in the M-Si-N₂ systems. As some of the samples nitrated, they sintered and

formed a crust on the surface so that the samples were not homogeneous in nitrogen throughout. More useful results would be obtained by introducing nitrogen into the system in the form of a metal nitride. The preparation of Si_3N_4 and Ta_2N were investigated for this purpose.

In order to prepare Si_3N_4 , Si metal powder was heated in a Mo crucible under about $3/4$ atm of N_2 . The rate of the nitriding reaction was found to be very slow below 1600°K while above 1900°K Si_3N_4 showed considerable decomposition.

The heating schedule used was to first heat the sample at 1660°K for about 40 minutes, increase the temperature to 1800°K for about 20 minutes and then cool. The sintered portions of the resulting sample were then crushed and the sample was reheated to 1840°K for 110 minutes. The final sample was grayish-white in color. It contained 91 mol % Si_3N_4 as determined by gain in weight of the sample assuming no loss of Si due to vaporization or reaction with the container. Since there was actual loss due to these processes 91% is a minimum analysis. X-ray analysis showed a strong Si_3N_4 phase³⁵ plus a weak Si phase.

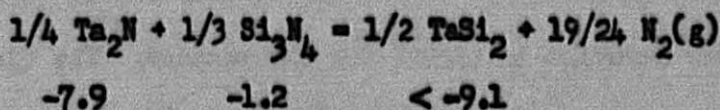
Ta_2N was prepared by heating Ta powder contained in a Mo crucible to 2100°K for 33 minutes under $3/4$ atm of N_2 . From the weight gain the composition was calculated to be $\text{Ta}_{1.96}\text{N}$. The x-ray diffraction pattern showed Ta_2N as a single phase.

Work on the N-Si- N_2 systems was concentrated on the Ta-Si- N_2 system with only a few reactions in the other systems being studied. A summary of the reactions and the resulting phases is presented in Table XI.

Ternary compounds of the Mn_5Si_3 type appeared in the Nb-Si- N_2 and Ta-Si- N_2 systems. Insufficient work was done on the other systems to indicate the presence of ternary compounds.

Heatings at 1600°K in the Ta-Si-N₂ system show that TaSi₂ is unstable in the presence of N₂ and will react to give Ta₅Si₃N_x. Si₃N₄ would also be expected to form, however it was not picked up by x-ray analysis. When samples of Si content 38% and lower, were heated in N₂ at 1600°K they showed a considerable gain in weight. The phase Ta₂N appeared in equilibrium with Ta₅Si₃N_x. Some weak unidentified lines were also present. These lines may be due to TaN. From these data a provisional form of the Ta-Si-N₂ diagram has been constructed at 1600°K (see Figure VII).

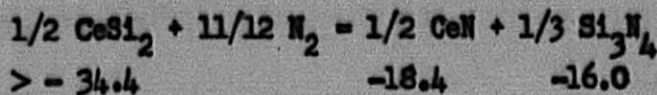
At 2146°K TaSi₂ was found to be stable in the presence of N₂. This means that the following reaction can proceed as written. The ΔF_T^o of formation



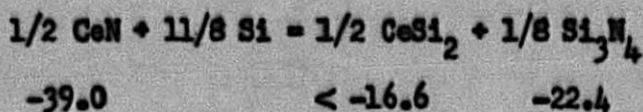
of Ta₂N and Si₃N₄ have been indicated in the equation. This means that ΔH₂₉₈^o of formation for TaSi₂ is less than -9.1 kcal. This does not improve the limits already set for TaSi₂ however a study of the equilibrium at a lower temperature would give additional data.

The Nb-Si-N₂ system appears to be similar to the Ta-Si-N₂ system. Joins were established between Nb₅Si₃N_x and N₂ and between Nb₅Si₃N_x and NbSi₂.

From the gain in weight and physical appearance of a sample resulting from Ce plus 2Si plus N₂, it is evident that CeSi₂ is unstable in the presence of N₂. The x-ray pattern was too poor to reveal anything. Providing that no ternary compounds are formed in the Ce-Si-N₂ system, the following reaction can proceed at 1610°K. From a calculation of ΔF_T^o for CeN and Si₃N₄, we



can set an upper limit for ΔH_{298}° of formation of CeSi_2 as greater than -34.4 kcal. per equivalent of Si. Since there was no attack of the container by Si, it is assumed that a join exists between CeSi_2 and Si_3N_4 so that the reaction



can go as written. Assuming $\Delta S_{298}^\circ = 0$ for this reaction we obtain a lower limit for the ΔH_{298}° of formation of CeSi_2 as less than -16.6 kcal. per equivalent of Si. These calculations are, of course, provisional.

In the Ti-Si-N₂ system a sample containing 62% Ti and 38% Si reacted with N₂ to give TiN. No other phases were found. A sample initially containing 69% Si showed considerable attack of the Mo container yielding TiN plus an unidentified phase.

When a sample containing 33% Zr and 67% Si was heated in N₂ in a Mo crucible it yielded the phases MoSi₂, ZrN and ZrSi₂ plus weak unidentified lines. Crucible attack would be expected since ZrSi₂ was previously found to be unstable in the presence of Mo. When Zr metal was heated with excess Si₃N₄ in a ZrO₂ container in the presence of N₂ at 2100°K, an unidentified phase of strong intensity appeared along with Si metal. The Si metal came from decomposition of the Si₃N₄. The unknown phase may be a ternary compound.

$M_1 - M_2 - Si$ SYSTEMS

In the $M_1 - M_2 - Si$ systems it is difficult to obtain thermodynamic data from the phases observed because of extended solid solubilities in these systems. Nevertheless some useful data were obtained. The main region studied was that of low Si content. A summary of the heatings is given in Table XII.

It was established that all of the lower silicides of Ta are stable in the presence of Mo metal.

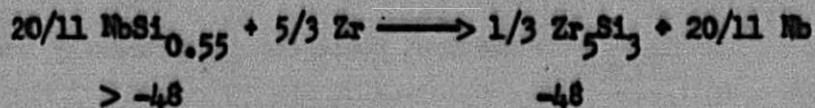
Ta_2Si and $TaSi_{0.2}$ were also found to be stable in the presence of W.

A join was found to exist between Ta_2Si and Ti_5Si_3 . The lattice constants of Ti_5Si_3 were expanded indicating a solubility of Ta in Ti_5Si_3 .

Mo will reduce $TiSi_2$ to Ti_5Si_3 . Ti_5Si_3 is believed to be stable in the presence of Mo. It is believed that a join exists between Ti_5Si_3 and $MoSi_2$.

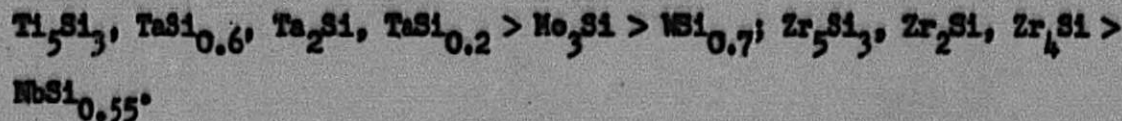
Mo_3Si was found to be stable in the presence of W with no apparent change in lattice constants of either phase.

A join exists between Zr_5Si_3 and Nb. Nb_5Si_3 and Zr_5Si_3 appear to be completely soluble in each other. X-ray analysis of the region showed a phase of the Mn_5Si_3 structure with lattice constants intermediate between Nb_5Si_3 and Zr_5Si_3 . The following reaction should proceed as written:



This additional information is entered in Table IX.

The relative stability of the silicides may be summarized as follows:



DISCUSSION OF RESULTS

A consideration of the stabilities of the lower silicides only, shows that the most stable silicides occur in the same region of the periodic table as do the most stable carbides, i.e., Ti, Zr and Ta apparently form the most stable silicides as well as the most stable carbides. The stability region falls off toward the alkali metals or toward the iron and platinum metals. The most stable silicides are more stable than the most stable carbides, and silicides exhibit a wider range of stability over the periodic table. This is to be expected since Si has a much lower heat of sublimation than C.

In considering the stabilities of the disilicides a trend in stability over the periodic table is less pronounced. Various values that have been reported for ΔH_{298}° of formation of disilicides are CaSi_2 , -18;²⁶ ZrSi_2 , -21 (this work); ReSi_2 , -27.5;¹ and CoSi_2 , -12.3²⁶ kcal. per equiv. of Si.

Although the stability region of silicides is considerably more widespread than that of the carbides, we note that silicides are no longer stable as we go further in the periodic table, than Cu, Pd and Pt. We also find that d shells for the various atoms have been filled at this point. This suggests that d electrons play an important role in the bonding of the silicides.

The Mn_5Si_3 type structure seems to be a very important crystal type in the refractory silicides since some of the most stable and highest melting silicides appear to be these of the Mn_5Si_3 structure. In case this structure is absent in the binary system a small amount of C (or possibly N or O) is sufficient to stabilize it. Also, with the exception of $\text{Ta}_{4.8}\text{Si}_3\text{C}_{0.5}$ these Mn_5Si_3 type compounds all appear to have an appreciable homogeneity range.

The crystal structures of many of the important lower silicides have not yet been determined. Among these are the Zr_4Si_3 , Zr_6Si_5 , $TaSi_{0.6}$, $TaSi_{0.2}$, Mo_3Si_2 and $WSi_{0.7}$ phases.

The disilicides appear to exhibit a variety of structures: $TiSi_2$ being of the C_{54} type;³⁶ $ZrSi_2$, C_{49} ,³⁷ $NbSi_2$ and $TaSi_2$, C_{40} ,³⁷ $MoSi_2$, WSi_2 and $ReSi_2$, C_{20} ,³⁷ and $CeSi_2$, $\alpha ThSi_2$.¹³

The melting points of the silicides follow the same general trend found with the carbides except that the melting points are about 1000° lower. The melting points of both silicides and carbides appear to increase as we go to higher members of a group. The melting points of W and Mo silicides are found to be relatively high as compared to the trend found with the carbides. This agrees with the fact that the Mo and W silicides appear to be more stable than the carbides. The highest melting silicides have been reported as Ti_5Si_3 , 2390°K;⁸ Zr_6Si_5 , 2520°K;⁹ Nb_5Si_3 , >2230°K (this work); $Ta_{4.5}Si$, 2780°K;³⁸ Mo_3Si_2 , 2470°K;²⁷ and $WSi_{0.7}$, 2610°K.³⁹

ACKNOWLEDGMENTS

The x-ray diffraction films were prepared by Mrs. Helena Rubin and interpreted by Mrs. Carol Dauben. The authors would like to express their appreciation for this help which was essential for this work. The authors would also like to thank Dr. John Conway for spectroanalysis of starting materials and Mrs. Jane Waite for typing the manuscript.

This work was performed under the auspices of the U. S. Atomic Energy Commission.

TABLE I

Compound	Structure Type	Lattice Constants	Temperature of Preparation
Zr ₅ Si ₃ *	Mn ₅ Si ₃	a = 7.940 ± 0.008A** c = 5.553 ± 0.006A	1691-2141°K
		a = 7.958 ± 0.005A*** c = 5.564 ± 0.005A	
Zr ₂ Si		a = 6.646 ± 0.008A c = 5.300 ± 0.008A	1691-1952°K
Zr ₄ Si			1952°K
Nb ₅ Si ₃	Mn ₅ Si ₃	a = 7.547 ± .005A c = 5.240 ± .005A	2095-2201°K
NbSi _{0.55}	(TaSi _{0.6})		1937-2201°K
CeSi ₂	αThSi ₂	a = 4.175 ± .002A c = 13.848 ± .006A	1605°K
CeSi			1605-1691°K
Ce ₂ Si			1625°K
Ce ₃ Si			1625-1691°K
Nb ₂ C	Ta ₂ C	a = 3.117 ± .003A c = 4.969 ± .005A	1920-2130°K
Ce ₂ C ₃	Pu ₂ C ₃	a = 8.455 ± .008A	1673°K
CeC	NaCl	a = 5.130 ± .002A	1673°K
CeC ₂			2195°K
Zr ₅ Si ₃ C _x *	Mn ₅ Si ₃		1920°K
Nb ₅ Si ₃ C _x *	Mn ₅ Si ₃		2130°K
Ta _{4.8} Si ₃ C _{0.5}	Mn ₅ Si ₃	a = 7.494 ± .007A c = 5.242 ± .007A	2071-2142°K
Mo ₄ CSi ₃ *	Mn ₅ Si ₃	a = 7.285 ± .007A**** c = 5.242 ± .007A	2071-2169°K
Ta ₂ N			2104°K
Ta ₅ Si ₃ N _x *	Mn ₅ Si ₃		1602-2365°K
Nb ₅ Si ₃ N _x *	Mn ₅ Si ₃		2109-2146°K

*Compound exhibits an appreciable homogeneity range.

**Lattice constants are given for a sample containing 40.4% Si.

***Lattice constants are for the sample furnished by Dr. McPherson. The sample contains 35.1% Si.

****Lattice constants are given for the composition Mo₄CSi₃.

TABLE II

Ti - Si System

Sample Number	Atomic % Si	Final Temp. (°K)	Time (min.)	Description of Sample	Phases Observed
209	17.8	2105	20	Fused cruc. attack	$\frac{\text{Mo}}{\text{m.s.}} + \frac{\text{Ti}_5\text{Si}_3^*}{\text{m.w.}}$
67	20.2	1691	17	Fused	$\frac{\text{Ti}_5\text{Si}_3}{\text{s.}} + \frac{\text{Ti}}{\text{v.w.}}$
22	30.0	2105	20	Fused	$\frac{\text{Ti}_5\text{Si}_3}{\text{s.}} + \frac{\text{Mo}}{\text{v.w.}}$
20	33.5	2105	20	Sintered Porous	$\frac{\text{Ti}_5\text{Si}_3}{\text{s.}}$
23	37.5	2105	20	Partially fused	$\frac{\text{Ti}_5\text{Si}_3}{\text{s.}}$
112	50.5	1933	30	Partially fused	$\frac{\text{Ti}_5\text{Si}_3}{\text{m.}} + \frac{?}{\text{w.}}$
21	50.5	2105	20	Fused	$\frac{\text{Ti}_5\text{Si}_3}{\text{s.}} + \frac{?}{\text{w.}}$
81	60.0	2141	25	Fused	$\frac{\text{Ti}_5\text{Si}_3}{\text{s.}} + \frac{?}{\text{v.w.}}$
143	60.2	1870 (max. temp. 2190)	65	Fused Al ₂ O ₃ cruc. crystals above melt	$\frac{\text{TiSi}_2}{\text{s.}} + \frac{\text{Ti}_5\text{Si}_3}{\text{w.}}$
24	67.1	2105	20	Fused	$\frac{\text{MoSi}_2}{\text{s.}} + \frac{\text{Ti}_5\text{Si}_3}{\text{w.}}$
111	71.9	1597 (max. temp. 1618)	54	Partially fused	$\frac{\text{TiSi}_2}{\text{m.}} + \frac{\text{Si}}{\text{w.}}$

*Relative intensities of lines have changed considerably.

TABLE III

Zr - Si System

Sample Number	Atomic % Si	Final Temp. (*K)	Time (min.)	Description of Sample	Phases Observed
197	22.4	1952	62	Fused condensate on walls	<u>A phase</u> m.
198	35.0	1952	62	Partially fused	$\frac{\text{Zr}_2\text{Si}}{m.} + \frac{\text{Zr}_5\text{Si}_3}{w.}$
199	40.4	1952	62	Sintered	$\frac{\text{Zr}_2\text{Si}}{m.s.} + \frac{?}{v.w.}$
203*	40.4	2094 (Max. temp. 2156)	34	Well sintered brown color on surface	$\frac{\text{Zr}_5\text{Si}_3}{m.s.}$
200	42.6	1952	62	Sintered	$\frac{\text{Zr}_2\text{Si}}{m.s.} + \frac{\text{Zr}_5\text{Si}_3}{w.} + \frac{?}{w.}$
204*	42.6	2094 (Max. temp. 2156)	34	Slightly sintered brown color on surface	$\frac{\text{Zr}_5\text{Si}_3}{m.s.} + \frac{\text{Zr}_4\text{Si}_3}{w.}$
201	45.4	1952	62	Sintered	$\frac{\text{Zr}_2\text{Si}}{m.s.} + \frac{?}{w.}$
205*	45.4	2094 (Max. temp. 2156)	34	Not sintered	$\frac{\text{Zr}_5\text{Si}_3}{m.} + \frac{\text{Zr}_6\text{Si}_5}{m.} + \frac{\text{Zr}_4\text{Si}_3}{w.}$
205a*	45.4	2094 (Max. temp. 2156)	34	Sintered	$\frac{\text{Zr}_5\text{Si}_3}{m.} + \frac{\text{Zr}_6\text{Si}_5}{m.} + \frac{\text{Zr}_4\text{Si}_3}{w.} + \frac{?}{w.}$
202	49.8	1952	62	Sintered	$\frac{\text{ZrSi}}{m.s.} + \frac{\text{Zr}_2\text{Si}}{m.w.}$
206*	49.8	2094 (Max. temp. 2156)	34	Not sintered Brown color on surface	Prob. a mixture of Zr_6Si_5 , Zr_5Si_3 and ZrSi

*Preceding sample reheated.

TABLE IV

Er - Si - O System

Sample Number	Atomic % Si	Atomic % O	Final Temp. (*K)	Time (min.)	Description of Sample	Phases Observed
113	14.4	18.3	1933	30	Sintered. Brown color on surface	Er° + $\frac{\text{Er}_2\text{Si}_3}{\text{n.}}$
119	14.4	18.3	1997	25	Sintered. Brown color on surface	Er° + $\frac{\text{Er}_2\text{Si}_3}{\text{n.s.}}$
68	18.8	16.3	1691	17	Sintered	Er° + $\frac{\text{Er}_2\text{Si}_3}{\text{n.}}$
85	18.8	16.8	2141	25	Partially fused crucible attack	$\frac{?}{\text{n.}}$
114	22.5	16.5	1933	30	Sintered. Brown color on surface	Er° + $\frac{\text{Er}_2\text{Si}_3}{\text{n.}}$
120	22.5	16.5	1997	25	Sintered	Er° + $\frac{\text{Er}_2\text{Si}_3}{\text{n.s.}}$
115	26.0	15.9	1933	30	Sintered. Brown color on surface	Er° + $\frac{\text{Er}_2\text{Si}_3}{\text{s.}}$
118	26.0	15.9	1997	25	Sintered. Brown color on surface	Er° + $\frac{\text{Er}_2\text{Si}_3}{\text{s.}}$
69	29.7	15.0	1691	17	Sintered	$\frac{\text{Er}_2\text{Si}_3}{\text{n.}}$ + $\frac{?}{\text{w.}}$

*Zr lattice largely expanded. Sample 115 showed the lattice constants

$a = 3.252 \pm 0.005\text{\AA}$ and $c = 5.216 \pm 0.005\text{\AA}$.

TABLE IV (cont.)

Sample Number	Atomic % Si	Atomic % O	Final Temp. (*K)	Time (min.)	Description of Sample	Phases Observed
86	29.7	15.0	2141	25	Sintered	$\frac{\text{Er}_2\text{Si}_2}{\text{n.s.}}$
116	32.7	14.3	1933	30	Sintered. Brown color on surface	$\frac{\text{Er}_2\text{Si}_2}{\text{n.s.}}$ + $\frac{\text{ErSi}}{\text{n.}}$ + $\frac{\text{?}}{\text{w.}}$
121	32.7	14.3	1997	25	Sintered	$\frac{\text{Er}_2\text{Si}_2}{\text{n.s.}}$ + $\frac{\text{ErSi}}{\text{n.}}$ + $\frac{\text{?}}{\text{w.}}$
82	35.5	13.6	2141	25	Sintered	$\frac{\text{Er}_2\text{Si}_2}{\text{n.s.}}$ + $\frac{\text{?}}{\text{n.}}$
117	38.2	13.3	1933	30	Sintered. Brown color on surface	$\frac{\text{ErSi}}{\text{n.}}$ + $\frac{\text{?}}{\text{w.}}$
122	38.2	13.3	1997	25	Sintered. Brown color on surface	$\frac{\text{ErSi}}{\text{n.}}$ + $\frac{\text{?}}{\text{n.v.}}$
70	47.2	11.3	1691	17	Sintered. Brown color on surface	$\frac{\text{ErSi}}{\text{n.}}$ + $\frac{\text{ErSi}_2}{\text{n.v.}}$
87	47.2	11.3	2141	25	Partially fused	$\frac{\text{ErSi}}{\text{n.s.}}$
83	55.0	9.6	2141	25	Partially fused Crucible attack	$\frac{\text{ErSi}}{\text{n.}}$ + $\frac{\text{ErSi}_2}{\text{v.}}$
144	55.4	9.5	1870 (Max. temp. 2192)	65	Partially fused Crucible attack	$\frac{\text{NoSi}_2}{\text{.}}$ + $\frac{\text{ErSi}}{\text{n.}}$ + $\frac{\text{?}}{\text{w.}}$
71	62.4	8.1	1691	17	Sintered	$\frac{\text{ErSi}_2}{\text{n.}}$
88	62.4	8.1	2141	25	Partially fused Crucible attack	$\frac{\text{ErSi}}{\text{n.s.}}$ + $\frac{\text{NoSi}_2}{\text{v.}}$

TABLE V
Ce - Si System

Sample Number	Atomic % Si	Final Temp. (*K)	Time (min.)	Phases Observed
74	17.4	1625 (Max. temp. 1765)	34	$\frac{\text{CeO}_2}{n.} + \frac{\text{Ce}_2\text{Si}}{v.}$
72	19.2	1691	17	$\frac{\text{CeO}_2}{n.} + \frac{\text{Ce}_2\text{Si}}{n.}$
75	26.0	1625 (Max. temp. 1765)	34	$\frac{\text{CeO}_2}{n.} + \frac{\text{Ce}_2\text{Si}}{n.}$
106	32.8	1617 (Max. temp. 1787)	44	$\frac{\text{Ce}_2\text{Si}}{n.}$
76	35.5	1625 (Max. temp. 1765)	34	$\frac{\text{Ce}_2\text{Si}}{n.}$
105	37.3	1617 (Max. temp. 1787)	44	$\frac{\text{Ce}_2\text{Si}}{n.}$ †
107	39.8	1617 (Max. temp. 1787)	44	$\frac{\text{CeSi}_2}{n.} + \frac{\text{CeSi}}{v.}$
77	43.0	1605 (Max. temp. 1779)	44	$\frac{\text{CeSi}}{n.}$
73	50.0	1691	17	$\frac{\text{CeSi}_2}{n.} + \frac{\text{CeSi}}{v.}$
78	66.9	1605 (Max. temp. 1779)	44	$\frac{\text{CeSi}_2}{n.}$

All samples were partially fused.

TABLE VI

Nb - Si System

Sample Number	Atomic % Si	Final Temp. (*K)	Time (min.)	Description of Sample	Phases Observed
3	13.0	2095	13	Sintered	$\frac{\text{Nb}}{\text{s.}}$ + $\frac{\text{NbSi}_{0.55}}{\text{v.}}$ + $\frac{\text{Nb}_5\text{Si}_3}{\text{v.v.}}$
221	16.7 (Max. temp. 1986)	1937	45	Sintered	$\frac{\text{Nb}}{\text{n.s.}}$ + $\frac{\text{NbSi}_{0.55}}{\text{n.v.}}$
4	19.9	2095	13	Sintered	$\frac{\text{Nb}}{\text{s.}}$ + $\frac{\text{NbSi}_{0.55}}{\text{n.v.}}$
222	25.6 (Max. temp. 1986)	1937	45	Sintered	$\frac{\text{Nb}}{\text{n.}}$ + $\frac{\text{NbSi}_{0.55}}{\text{n.}}$
5	26.2	2095	13	Sintered	$\frac{\text{Nb}}{\text{n.}}$ + $\frac{\text{NbSi}_{0.55}}{\text{v.}}$
6	31.0	2095	13	Sintered	$\frac{\text{Nb}}{\text{n.}}$ + $\frac{\text{NbSi}_{0.55}}{\text{v.}}$ + $\frac{\text{Nb}_5\text{Si}_3}{\text{v.v.}}$
100	31.0 (Max. temp. 2231)	2201	26	Fused	$\frac{\text{NbSi}_{0.55}}{\text{n.}}$ + $\frac{\text{I}}{\text{v.}}$
7	35.6	2095	13	Sintered	$\frac{\text{Nb}}{\text{n.s.}}$ + $\frac{\text{NbSi}_{0.55}}{\text{n.v.}}$
101	38.0 (Max. temp. 2231)	2201	26	Partially fused	$\frac{\text{Nb}_5\text{Si}_3}{\text{n.}}$ + $\frac{\text{I}}{\text{v.}}$
8	39.5	2095	13	Sintered	$\frac{\text{Nb}}{\text{n.}}$ + $\frac{\text{NbSi}_{0.55}}{\text{n.v.}}$ + $\frac{\text{Nb}_5\text{Si}_3}{\text{v.}}$
65	50.1	2132	20	Fused	$\frac{\text{Nb}_5\text{Si}_3}{\text{s.}}$ + $\frac{\text{NbSi}_2}{\text{v.}}$
9	66.0	2095	13	Sintered	$\frac{\text{NbSi}_2}{\text{n.s.}}$ + $\frac{\text{Nb}_5\text{Si}_3}{\text{v.}}$ + I
63	76.2	2132	20	Sintered Crucible attack	$\frac{\text{NbSi}_2}{\text{v.s.}}$

TABLE VII

Heats and Entropies of Formation of Carbides

	ΔH_{298}° (kcal. per mole)	ΔS_{298}° (cal. per deg. per mole)
SiC	-13.0 ± 1.0	-1.90 ± 0.06
TiC	-43.85 ± 0.4	-2.81 ± 0.1
ZrC	-44.4 ± 1.1	-2.6 ± 1
NbC	-30 ± 5	-1.4 ± 1
TaC	-38.5 ± 0.6	-1.19 ± 0.1
Ta ₂ C	-36 ± 8	1.4 ± 1
MoC	-2.0 ± 0.7	0.0 ± 1
Mo ₂ C	-4.2 ± 1.1	2.4 ± 1
WC	-8.41 ± 0.2	1.5 ± 1
W ₂ C	-13 ± 4	5 ± 1

TABLE VIII

	S°	S°_{M}	S°_{C}
SiC	3.95	8.1	-4.1
TiC	5.79	9.8	-4.0
VC	6.77	10.1	-3.3
TaC	10.11	14.9	-4.8
$1/2 Cr_3C_2$	10.18	15.3	-5.1
$1/3 Cr_7C_3$	16.0	23.8	-7.8
Mn_3C	23.6	30.9	-7.3
Fe_3C	24.2	31.2	-7.0
B_4C	6.47	19.6	-13.1
Cr_6C	25.3	40.8	-15.5

TABLE IX

 ΔH_{298}° of Formation

$1/2 \text{TiSi}_2$	< -15.4	> -34.9	$5/3 \text{TaSi}_{0.6}$	< -12.8	> -77.2
$1/3 \text{Ti}_5\text{Si}_3$	< -15.4	> -86.1	Ta_2Si	< -12.8	> -90.1
$1/2 \text{ZrSi}_2$	-21 \pm 5		$\text{Ta}_{4.5}\text{Si}$	< -12.8	> -206
ZrSi	-39 \pm 10		$1/3 \text{Ta}_{4.8}\text{Si}_3\text{C}_{.5}$	< -12.8	> -74.7
$1/5 \text{Zr}_6\text{Si}_5$	-43 \pm 10		$1/2 \text{MoSi}_2$	-13 \pm 5	
$1/3 \text{Zr}_4\text{Si}_3$	-45 \pm 10		$1/2 \text{Mo}_3\text{Si}_2$	< -8.8	> -54.3
$1/3 \text{Zr}_5\text{Si}_3$	-48 \pm 10		Mo_3Si	< -8.8	> -109
Zr_2Si	-50 \pm 10		$1/3 \text{Mo}_4\text{CSi}_3$	< -9.2	> -52.6
Zr_4Si	-53 \pm 10		$1/2 \text{WSi}_2$	< -1.6	> -17.2
$1/2 \text{CeSi}_2$	< -16.6	> -34.4	$10/7 \text{WSi}_{0.7}$	< -4.6	> -25.0
$1/2 \text{NbSi}_2$	< -8.5	> -28	$1/2 \text{ReSi}_2$	-27.5*	
$1/3 \text{Nb}_5\text{Si}_3$	< -8.5	> -48	ReSi	-26.6*	
$20/11 \text{NbSi}_{0.55}$	< -8.5	> -48	Re_3Si	-21.2*	
$1/2 \text{TaSi}_2$	< -12.8	> -32.3			

*From the work of Searcy and McNeess.¹

TABLE I

Heats and Entropies of Formation of Nitrides

	ΔH_{298}° (kcal. per mole)	ΔS_{298}° (cal. per deg. per mole)
$1/4 \text{ Si}_3\text{N}_4$	-44.8	-20.4
TiN	-80.47 ± 0.3	-22.9
ZrN	-94.90	-22.9
CeN	-78.0	-25.6
TaN	-58.1	-20.6
Ta ₂ N	-72.4 ± 5	-19
NbN	-59	-21.4

-45-
TABLE XI

UCRL-2544

Sample No.	Reactants	Cruc.	Final Temp. (*K)	Time (min.)	Weight Change	Description of Sample	Phases Observed
194	Ti + 0.61 Si + N ₂	ZrO ₂	2109	20	-4.0%	Not sintered gold color	TiN s.
90	Ti + 2.18 Si + N ₂	Mo	2146	25	Un- known	Partially fused gold color Crucible attack	? m.s. + TiN m.s.
91	Zr + 2.04 Si + N ₂	Mo	2146	25	Un- known	Partially fused gold color Crucible attack	MoSi ₂ + ZrN v.s. + s. ZrSi ₂ + ? w. + v.w.
193	Zr + 13.1 Si ₃ N ₄ + N ₂	ZrO ₂	2109	20	-54%	Not sintered	? + Si s. + m.s.
102	Ce + 2.23 Si + N ₂	Mo	1610 (Max. temp. 1875)	36	13.5%	Black brittle solid. Strong odor of NH ₃	? v.w.
192	Nb + 0.60 Si + N ₂	ZrO ₂	2109	20	-0.2%		Nb ₅ Si ₃ N _x m.s.
99	Nb + 1.17 Si + 0.28 Si ₃ N ₄ + N ₂	Ta	2365	8	Un- known	Fused Crucible attack	(Ta,Nb)Si ₂ m.s. + (Ta,Nb) ₅ Si ₃ N _x m.s. + (Ta,Nb)Si _{0.6} w.
92	Nb + 2.01 Si + N ₂	Mo	2146	25	Un- known	Partially fused Crucible attack	NbSi ₂ + m. Nb ₅ Si ₃ N _x + ? m. + w.
127	Ta + 0.20 Si + N ₂	Mo	1602	65	+4.2%	Sintered	Ta ₅ Si ₃ N _x + ? m. + m.w.
126	Ta + 0.40 Si + N ₂	Mo	1602	65	+3.7%	Sintered	Ta ₅ Si ₃ N _x + m.s. Ta ₂ N + ? m.w. + v.w.

TABLE XI (cont.)

Sample No.	Reactants	Cruc.	Final Temp. (*K)	Time (min.)	Weight Change	Description of Sample	Phases Observed
125	Ta + 0.61 Si + N ₂	Mo	1602	65	+4.3%	Sintered	$\frac{\text{Ta}_5\text{Si}_3\text{N}_x}{\text{m.s.}}$ + $\frac{\text{TaSi}_2}{\text{m.}}$ + $\frac{?}{\text{w.}}$
98	Ta + 1.07 Si + 0.30 Si ₃ N ₄ + N ₂	Ta	2365	8	Un- known	Fused Crucible attack	$\frac{\text{TaSi}_2}{\text{m.}}$ + $\frac{\text{Ta}_5\text{Si}_3\text{N}_x}{\text{m.}}$ + $\frac{\text{TaSi}_{0.6}}{\text{v.w.}}$
138	Ta + 1.13 Si + 1.72 Si ₃ N ₄ + N ₂	Mo	1651	47	+5.5%	Not sintered	$\frac{\text{TaSi}_2}{\text{m.}}$ + $\frac{\text{Ta}_5\text{Si}_3\text{N}_x}{\text{m.}}$ + $\frac{\text{Ta}_2\text{N}}{\text{w.}}$
89	Ta + 2.20 Si + N ₂	Mo	2146 (Max. temp. 2182)	25	Un- known	Partially fused	$\frac{\text{TaSi}_2}{\text{v.s.}}$
124a	Ta + 2.30 Si + N ₂	Mo	1602	65	+7.1%	Top of sample	$\frac{\text{TaSi}_2}{\text{s.}}$ + $\frac{\text{Si}}{\text{m.}}$ + $\frac{?}{\text{v.w.}}$
124b	Ta + 2.30 Si + N ₂	Mo	1602	65	+7.1%	Bottom of sample	$\frac{\text{TaSi}_2}{\text{s.}}$ + $\frac{\text{Ta}_5\text{Si}_3\text{N}_x}{\text{m.}}$
139	TaSi _{2.30} N _{1.24} + N ₂	Mo	1651	47	+3.0%	124 reheated	$\frac{\text{TaSi}_2}{\text{s.}}$ + $\frac{\text{Ta}_5\text{Si}_3\text{N}_x}{\text{m.s.}}$ + $\frac{\text{Ta}_2\text{N}}{\text{w.}}$

TABLE XI (cont.)

Sample No.	Reactants	Cruc.	Final Temp. (*K)	Time (min.)	Weight Change	Description of Sample	Phases Observed
195	Ta ₂ N + 0.81 Si ₃ N ₄ + N ₂	Mo	2109	20	-14.1%	Sintered	TaSi ₂ s. + Ta ₅ Si ₃ N _x m.s.

TABLE XII

 $M_1 - M_2 - Si$ Systems

Sample Number	Atomic % M_1	Atomic % M_2	Atomic % Si	Atomic % O	Final Temp. ($^{\circ}K$)	Time (min.)	Description of Sample	Phases Observed
190	40.3-Ti	39.1-Zr	7.1	12.5	2071	22	Partially fused	$\frac{?}{m.}$
136	34.0-Ti	32.7-Zr	22.8	10.5	1995	32	Partially fused	$\frac{(Ti,Zr)_5Si_3}{m.} + \frac{?}{v.w.}$
171	51.0-Ti	15.5-Ta	31.1	2.4	2142	20	Partially fused	$\frac{(Ti, Ta)_5Si_3}{s.}$
191	30.6-Ti	30.9-Ta	37.0	1.5	2071	22	Partially fused	$\frac{Ti_5Si_3}{s.} + \frac{TaSi_4}{m.} + \frac{?}{v.w.}$
WTH-8-9	29.4-Ti	53.5-Mo	15.6	1.5	1920	30	Sintered	$\frac{Mo_3Si}{s.} + \frac{Mo}{s.} + \frac{?}{v.w.}$
WTH-8-10	27.4-Ti	18.9-Mo	52.3	1.4	1920	30	Sintered	$\frac{Ti_5Si_3}{m.s.} + \frac{(Ti, Mo)Si_2}{m.}$
135	33.9-Zr	35.3-Nb	21.5	9.3	1995	32	Sintered	$\frac{Zr_5Si_3}{m.} + \frac{Nb}{w.}$
187	29.7-Zr	31.1-Nb	31.2	8.0	2071	22	Partially fused	$\frac{(Nb, Zr)_5Si_3}{m.} + \frac{Nb}{m.}$
186	26.4-Zr	27.7-Nb	38.9	7.0	2071	22	Sintered	$\frac{ZrSi}{m.s.} + \frac{?}{m.}$
185	26.0-Zr	27.9-Ta	39.0	7.1	2071	22	Partially fused	$\frac{Ta_2Si}{m.s.} + \frac{Ta}{m.} + \frac{?}{m.}$

TABLE XII

 $M_1 - M_2 - Si$ Systems

Sample Number	Atomic % M_1	Atomic % M_2	Atomic % Si	Atomic % O	Final Temp. ($^{\circ}K$)	Time (min.)	Description of Sample	Phases Observed
137	37.5-Zr	39.2-Mo	13.2	10.1	1995	32	Sintered	$\frac{(Mo, Zr)}{m.} + \frac{?}{w.}$
173	33.5-Zr	34.6-Mo	23.0	8.9	2142	20	Sintered	$\frac{(Mo, Zr)}{s.} + \frac{?}{m.}$
WTH-8-13	7.7-Ce	77.0-Ta	15.3		1920	30	Sintered	$\frac{Ta_2Si}{m.} + \frac{CeO_2}{w.}$ + ?/v.w.
133	37.8-Nb	39.7-Mo	22.5		1995	32	Sintered	$\frac{Mo_3Si}{s.} + \frac{Mo_3Si_2}{w.}$
188	29.2-Nb	29.4-Mo	41.4		2071	22	Sintered	$\frac{(Mo, Nb)}{s.} + \frac{?}{m.}$
134	38.2-Nb	38.6-W	23.2		1995	32	Sintered	$\frac{W}{s.} + \frac{WSi_{0.7}}{m.}$
130	45.0-Ta	45.9-Mo	9.1		1983	30	Sintered	$\frac{(Mo, Ta)}{m.s.} + \frac{Ta_2Si}{m.}$
169	41.1-Ta	41.2-Mo	17.7		2142	20	Well-sintered	$\frac{Ta_2Si}{m.s.} + \frac{(Mo, Ta)}{m.}$ + ?/v.w.
170	38.4-Ta	38.4-Mo	23.2		2142	20	Well-sintered	$\frac{(Mo, Ta)}{s.} + \frac{(Mo, Ta)Si_{0.6}}{m.s.}$
129	44.25-Ta	46.75-W	9.0		1983	30	Sintered	$\frac{W}{m.s.} + \frac{Ta_2Si}{w.}$ + ?/v.w.
172	41.2-Ta	42.1-W	16.7		2142	20	Slightly sintered	$\frac{W}{s.} + \frac{(W, Ta)}{s.} + \frac{Ta_2Si}{m.s.}$

TABLE XII

 $M_1 - M_2 - Si$ Systems

Sample Number	Atomic % M_1	Atomic % M_2	Atomic % Si	Final Temp. (*K)	Time (min.)	Description of Sample	Phases Observed
189	33.2-Ta	33.2-W	33.6	2071	22	Well sintered	$\frac{W}{s.} + \frac{WSi_{0.7}}{m.} + \frac{Ta_2Si}{w.}$
128	41.7-Mo	43.7-W	14.6	1983	30	Sintered	$\frac{Mo_3Si}{s.} + \frac{W}{m.}$

REFERENCES

- (1) A. W. Searcy and R. A. McNeess, Jr., *J. Am. Chem. Soc.* 75, 1578 (1953).
- (2) L. Brewer, L. A. Bromley, P. W. Gilles and N. L. Lofgren, Declassified Atomic Energy Commission Report MDDC-367, August 4, 1945.
- (3) R. F. Domagala, D. J. McPherson and M. Hansen, "The Zirconium-Oxygen System," Armour Research Foundation of Illinois Institute of Technology, Report No. 4, Summary (COO-181), March 31, 1953.
- (4) E. S. Bumps, H. D. Kessler and M. Hansen, *Trans. Am. Soc. Metals* Preprint No. 32, (1952).
- (5) L. Brewer, A. W. Searcy, D. H. Templeton and C. H. Dauben, *J. Am. Ceram. Soc.* 33, 291 (1950).
- (6) H. Nowotny, H. Schachner, R. Kieffer and F. Benesovsky, *Monatsh.* 84, 1 (1953).
- (7) P. Pietrokowsky and P. Duwez, *J. Metals* 3, No. 9, Trans., 772 (1951).
- (8) M. Hansen, H. D. Kessler and D. J. McPherson, *Trans. Am. Soc. Metals* 44, 518 (1951).
- (9) C. E. Lundin, D. J. McPherson and M. Hansen, *Trans. Am. Soc. Metals* Preprint No. 41, (1952).
- (10) H. Schachner, H. Nowotny and R. Machenschalk, *Monatsh.* 84, 677 (1953).
- (11) William Hicks, Unpublished research, University of California, Berkeley, California.
- (12) L. Brewer, *Chemical Reviews* 52, 1 (1953).
- (13) G. Brauer and A. Metius, *Z. Anorg. Chemie* 249, 325 (1942).
- (14) W. H. Zachariasen, *Acta Cryst.* 2, 94 (1949).
- (15) G. Brauer and W. Scheele, *Fiat Review of German Science 1939-1946, Anorganische Chemie*, edited by W. Klemm, Vol. 24, Part II, Dietrich Verlagsbuchhdlg. Wiesbaden (1948).

REFERENCES

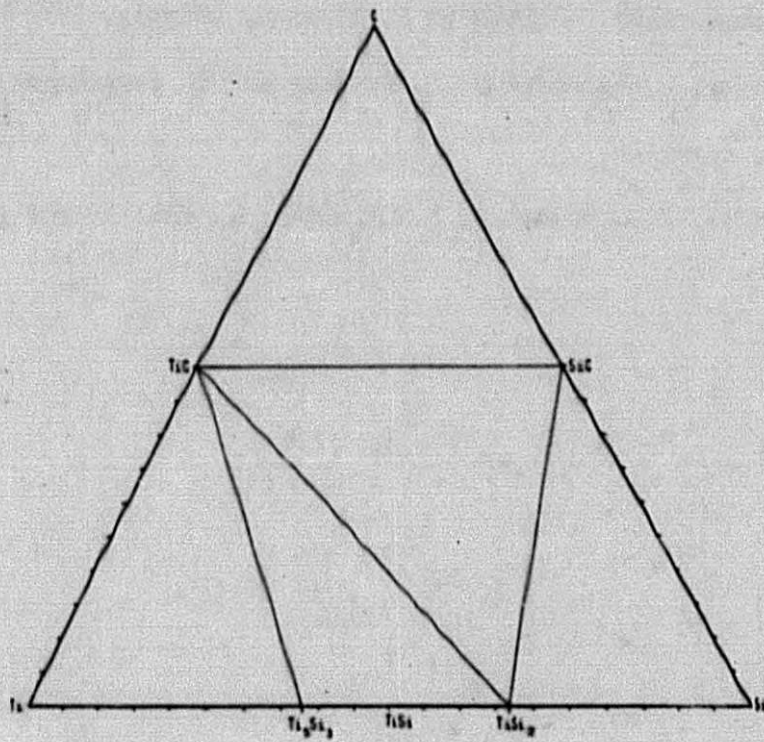
(2)

- (16) G. L. Humphrey, S. S. Todd, J. P. Coughlin and E. G. King, U. S. Bureau of Mines Report of Investigations 4888, July, 1952.
- (17) K. K. Kelley, U. S. Bureau of Mines Bulletin 477, (1950).
- (18) W. M. Latimer, "The Oxidation States of the Elements and Their Potentials in Aqueous Solutions," Second Edition, Prentice-Hall, New York, 1952.
- (19) G. L. Humphrey, J. Am. Chem. Soc. 73, 2261 (1951).
- (20) G. L. Humphrey, J. Am. Chem. Soc. 76, 978 (1954).
- (21) G. Huff, E. Squitieri and P. Snyder, J. Am. Chem. Soc. 70, 3380 (1948).
- (22) F. H. Ellinger, Trans. Am. Soc. Metals 31, 89 (1943).
- (23) L. Brewer, "The Chemistry and Metallurgy of Miscellaneous Materials-Thermodynamics," edited by L. L. Quill, McGraw-Hill Book Company, Inc., New York (1950).
- (24) L. C. Browning and P. H. Emmett, J. Am. Chem. Soc. 74, 4773 (1952).
- (25) K. K. Kelley, U. S. Bureau of Mines Bulletin No. 476 (1949).
- (26) U. S. Bureau of Standards, "Selected Values of Chemical Thermodynamic Properties," February, 1952.
- (27) R. Kieffer and E. Cerwenka, Z. Metallkunde 43, 101 (1952). The Mo-Si system by Kieffer and Cerwenka has been adjusted to agree with data obtained by Ham and Herzig - J. L. Ham and A. J. Herzig, Second Annual Report to Office of Naval Research, Misc 1951-132 (Climax Molybdenum Company of Michigan, 1951).
- (28) M. Hansen, "Der Aufbau der Zweistofflegierungen," Springer Verlag, Berlin (1936).
- (29) Carol Dauben, Private communication, 1953.
- (30) G. Brauer, Z. Elektrochem. 46, 397 (1940).

REFERENCES

(3)

- (31) J. S. Umanski, Zhur. Fiz. Chim. U.S.S.R. 14, 332 (1940).
- (32) K. K. Kelley, Private communication, 1952.
- (33) P. Chiotti, J. Am. Ceram. Soc. 35, 123 (1952).
- (34) R. E. Slade and G. I. Higson, Chem. News 108, 166 (1913).
- (35) W. C. Leslie, K. G. Carroll and R. N. Fisher, J. Metals 2, 204 (1952).
- (36) F. Laves and H. L. Wallbaum, Z. Krist. 101, 78 (1939).
- (37) "Strukturbericht," edited by K. Hermann, Leipzig, 1931-1940.
- (38) R. Kieffer, F. Benesovsky, H. Nowotny and H. Schachner, Z. Metallkunde 44, 242 (1953).
- (39) R. Kieffer, F. Benesovsky, E. Gallistl, Z. Metallkunde 43, 284 (1952).



Ti-Si-C SYSTEM

MU-6082

Figure 1.

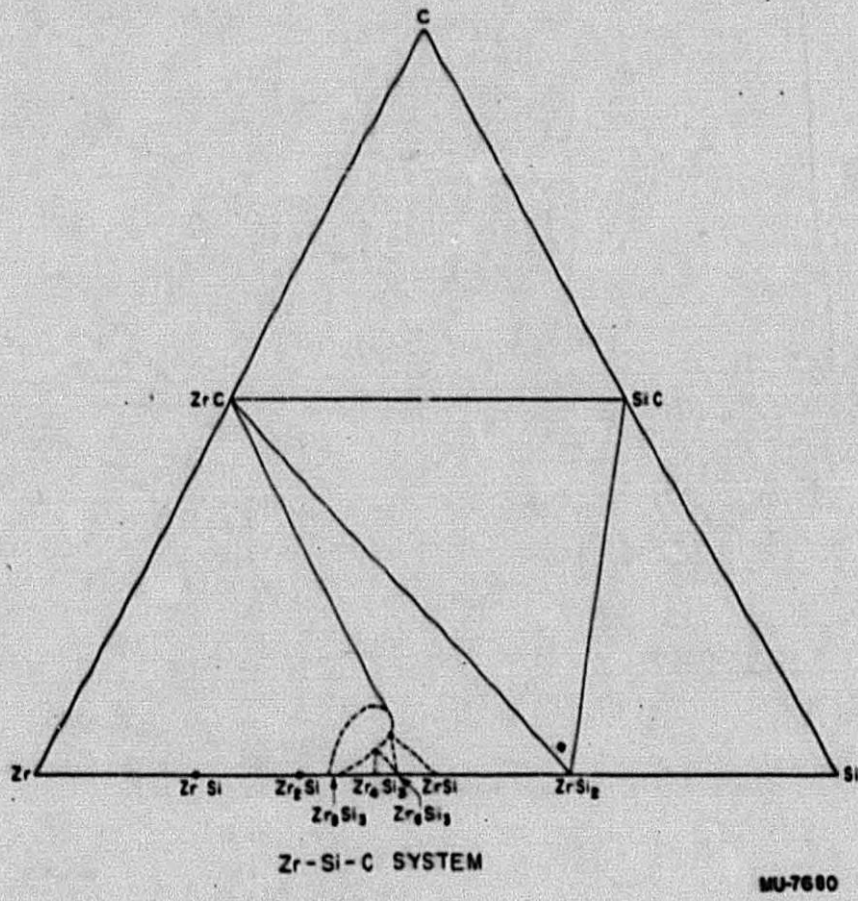
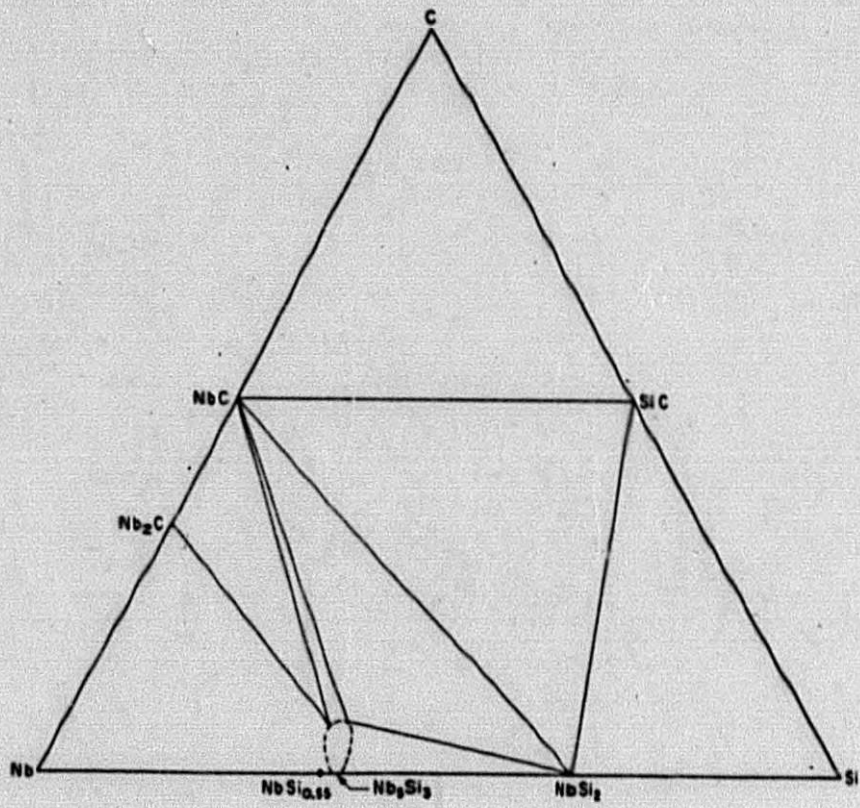


Figure II.



Nb-Si-C SYSTEM

MJ-7661

Figure III.

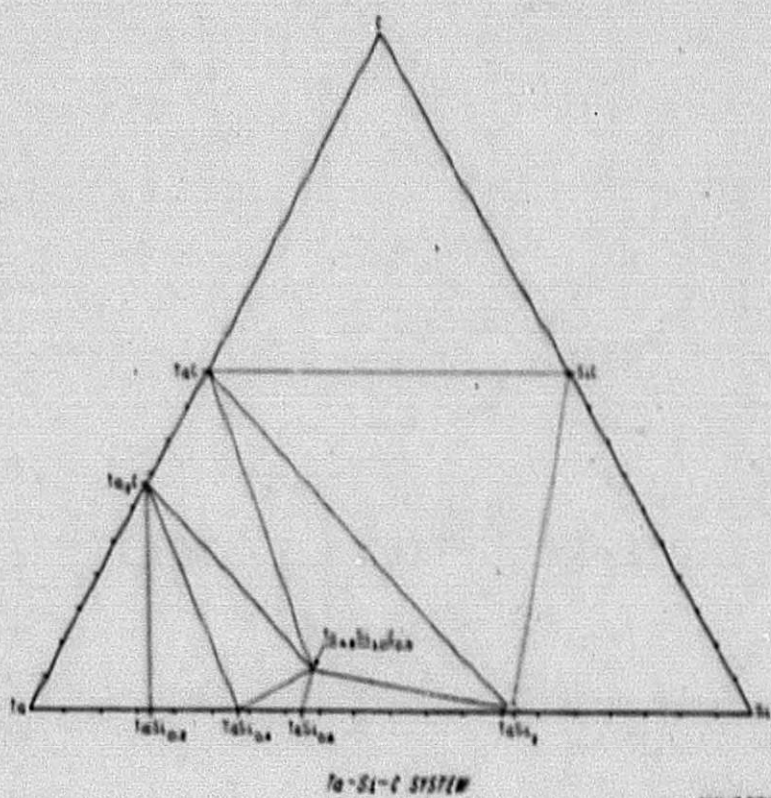
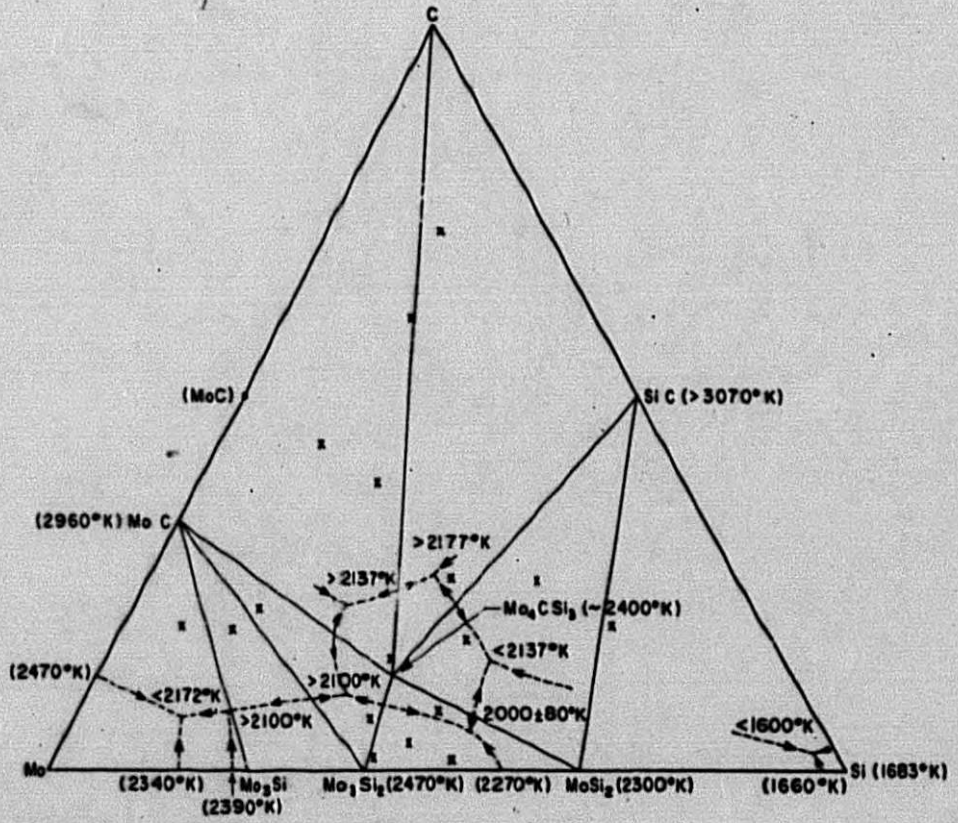


Figure IV.



Mo-Si-C SYSTEM
(BOUNDARIES ARE SCHEMATIC)

MU-7682

Figure V.

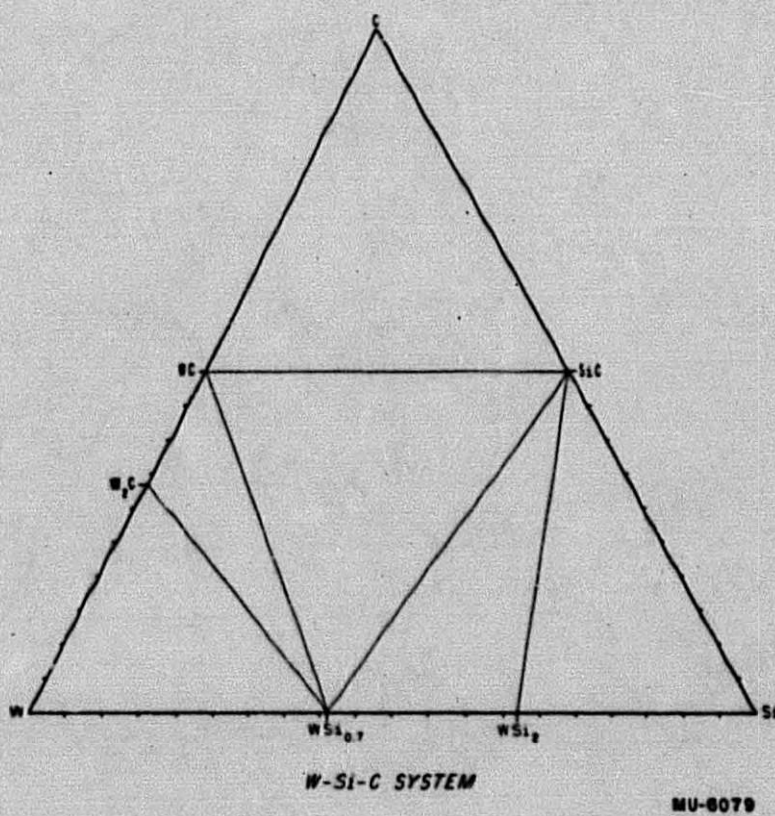
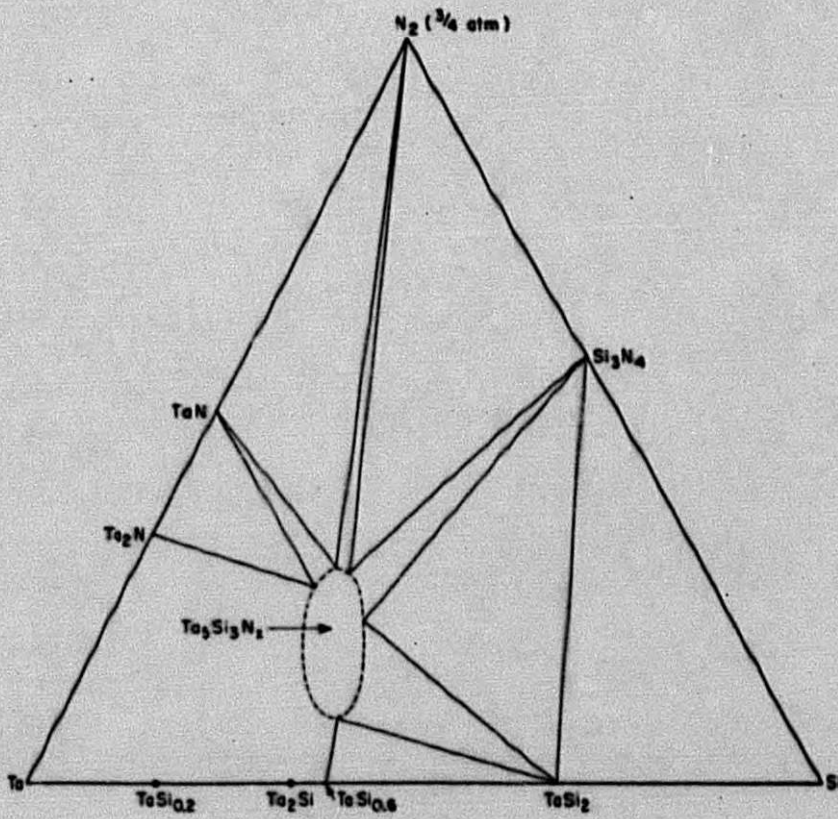


Figure VI.



Ta-Si-N₂ SYSTEM
(1600° K)

MU-7683

Figure VII.